

## Earth-Abundant Cobalt based photocatalyst: Visible light induced direct (Het)Arene C-H arylation and CO<sub>2</sub> capture

Pooja Rana,<sup>a</sup> Bhawna Kaushik,<sup>a</sup> Rashmi Gaur,<sup>a</sup> Sriparna Dutta,<sup>a</sup> Sneha Yadav,<sup>a</sup> Pooja Rana,<sup>a</sup> Kanika Solanki,<sup>a</sup> Bhavya Arora,<sup>a</sup> Ankush V. Biradar,<sup>b</sup> Manoj B Gawande,<sup>c</sup> and R. K. Sharma<sup>a\*</sup>

<sup>a</sup>Green Chemistry Network Centre, Department of Chemistry, University of Delhi, New Delhi-110007, India; Tel: 011-276666250; Email: [rksharmagreenchem@hotmail.com](mailto:rksharmagreenchem@hotmail.com)

<sup>b</sup>Inorganic Materials and Catalysis Division, CSIR-Central Salt and Marine Chemicals Research Institute, Bhavnagar 364002, Gujarat, India

<sup>c</sup>Institute of Chemical Technology Mumbai-Marathwada Campus, Jalna, 431213, Maharashtra, India.

### Abstract

In this work, we have reported a noble metal free heterogeneous photocatalyst to carry out direct (Het)Arene C-H arylation and solvent-free CO<sub>2</sub> capture *via* single-electron transfer processes at room temperature and pressure. The catalytic system comprises of a cobalt (III) complex grafted over the silica coated magnetic support for the efficient recovery of the photocatalytic moiety without hampering its light-harvesting capability. The novel earth-abundant cobalt (III) based photocatalyst possesses various fascinating properties such as high surface area to volume ratio, large pore volume, crystalline behaviour, high metal loading, excellent stability and reusability. General efficacy of the highly abundant and low-cost cobalt based heterogeneous nanocatalyst was checked for selective conversion of aryldiazonium salts into synthetically and pharmaceutically significant biaryl motifs under ambient conditions over irradiation with visible light. Highly efficient photocatalytic conversion of carbon dioxide (CO<sub>2</sub>) to value-added chemical was accomplished under mild reaction conditions with high selectivity, showing added benefit of operational simplicity.

## Table of Content

<b>1</b>	General Information	
<b>2</b>	Result and Discussion	
<b>3</b>	NMR Data	
<b>4</b>	GCMS DATA	
<b>5</b>	References	

## General Information

**Material Synthesis.** Unless otherwise indicated, all the chemicals were purchased from commercial source and were utilized without further purifications. Ferric sulphate hydrate and ferrous sulphate heptahydrate were obtained from Central Drug house and Thomas Bakers, respectively. The commercially unavailable substrates of benzene diazonium tetrafluoroborate derivatives were prepared in the lab utilizing the previously reported procedure.<sup>1</sup> All the photochemical reactions were carried out in inert atmosphere, unless otherwise indicated. The solvents *p*-xylene and DMSO were of analytical grade and purified by activated molecular sieves. Double distilled water was used for the synthetic procedure of material.

**Material Characterization.** The various physicochemical techniques were utilized to successfully characterise the fabricated Co@Apz@ASMNPs catalyst such as Fourier transform-infrared spectroscopy (FT-IR), powder X-ray diffraction (PXRD), UV-Vis spectroscopy, field emission-scanning electron microscopy (FE-SEM), high resolution-transmission electron microscopy (HR-TEM), vibrating sample magnetometry (VSM), Brunauer-Emmett-Teller analysis (BET), inductively coupled-plasma optical emission spectrometry (ICP-OES), X-ray photoelectron spectroscopy (XPS), energy-dispersive X-ray spectroscopy (EDS), energy-dispersive X-ray fluorescence (ED-XRF), and nuclear magnetic resonance spectroscopy (NMR). The Fourier transform-infrared spectra were investigated in the range of 4000 to 400 cm<sup>-1</sup> by employing PerkinElmer Spectrum 2000 using KBr pallet method. PXRD patterns were recorded to determine the phase, purity and crystalline nature on a Rigaku Cu (K<sub>α</sub>) diffractogram at a scan rate of 4 degree per min and 2θ range of 2-80 degree. UV-Vis spectrum of Co@Apz@ASMNPs has been investigated on a Thermo Scientific absorption spectrophotometer within the wavelength range of 250-800 nm. SEM images were captured on a Tescan MIRA3 FE-SEM microscope. SEM grids were prepared by dispersing the sample over a carbon tape placed on a SEM stub and further the nanoparticles were gold sputtered before image viewing. FEI TECHNAI G2 T20 transmission electron microscope operated at 200 KV was retain to capture the TEM images of the nanoparticles. The TEM samples of MNPs, SMNPs, Co@Apz@ASMNPs were prepared by drop casting method in which a sonicated ethanol suspension of the desired nanoparticles was drop cast over a carbon coated copper grid. Elemental analysis of the catalyst was acquired using an Ametek EDAX system. Brunauer-Emmett-Teller (BET) method was investigated using an ASI-CT-11 Quantachrome instrument at a degassing temperature of 180 °C to determine the specific surface area and pore volume. Cobalt loading/content of the Co@Apz@ASMNPs catalyst was quantitatively analysed by Perkin Elmer Avio 200 ICP-OES System. Magnetization of the nanoparticles were recorded using a vibrating sample magnetometer (EV-9, Microsense, ADE) in the range of -10000 Oe to 10000 Oe. <sup>1</sup>H NMR (400 MHz) and <sup>13</sup>C NMR (100 MHz) spectra were recorded on a JEOL JNM-EXCP 400 unless otherwise noted and data are reported in terms of chemical shift related to CDCl<sub>3</sub> (7.26 ppm) or with tetramethylsilane (TMS, δ 0.00 ppm) as the internal standard, abbreviation used to indicate the multiplicity (s = singlet, d = doublet, t = triplet, q = quartet, m = multiplet, dd = doublet of doublet, dt = doublet of triplet, ddd = doublet of doublet of doublet), coupling constant (Hz), integration. Thin-layer chromatography (TLC) was performed by utilizing Merck silica gel plates 60 F<sub>254</sub> to check the course of reactions and visualised under UV light.

Light Source. 12 W Philips white LED tube, Quantity of Light Source: Two

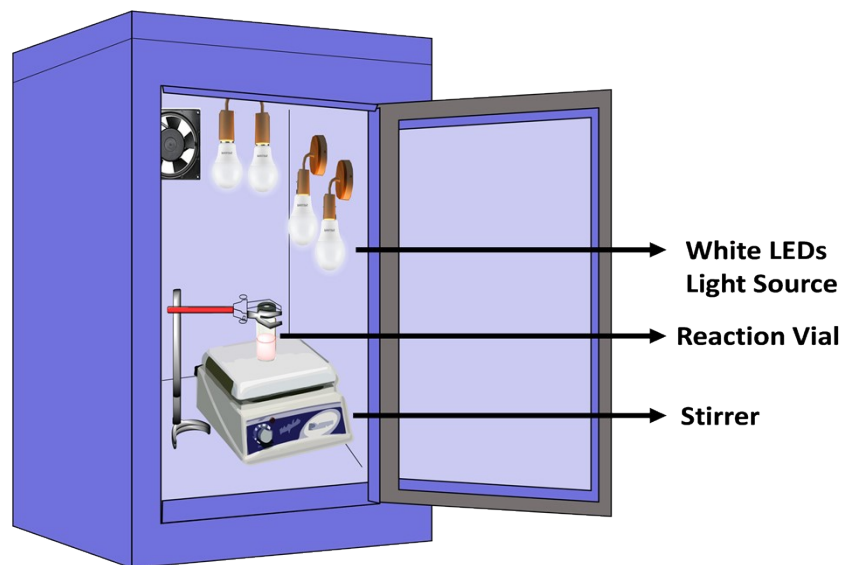


Figure 1. Photocatalytic reaction setup.

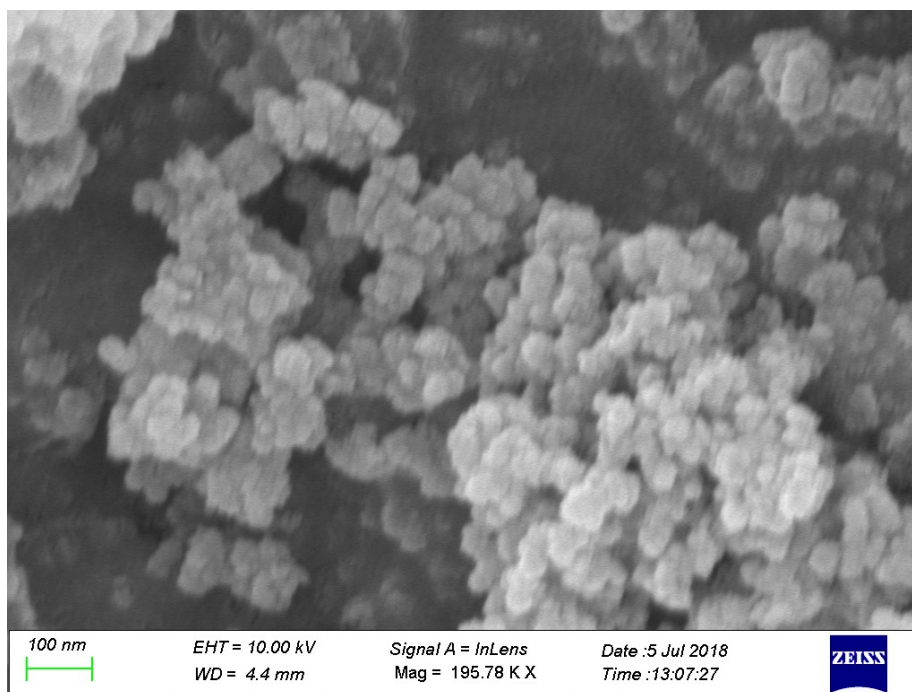
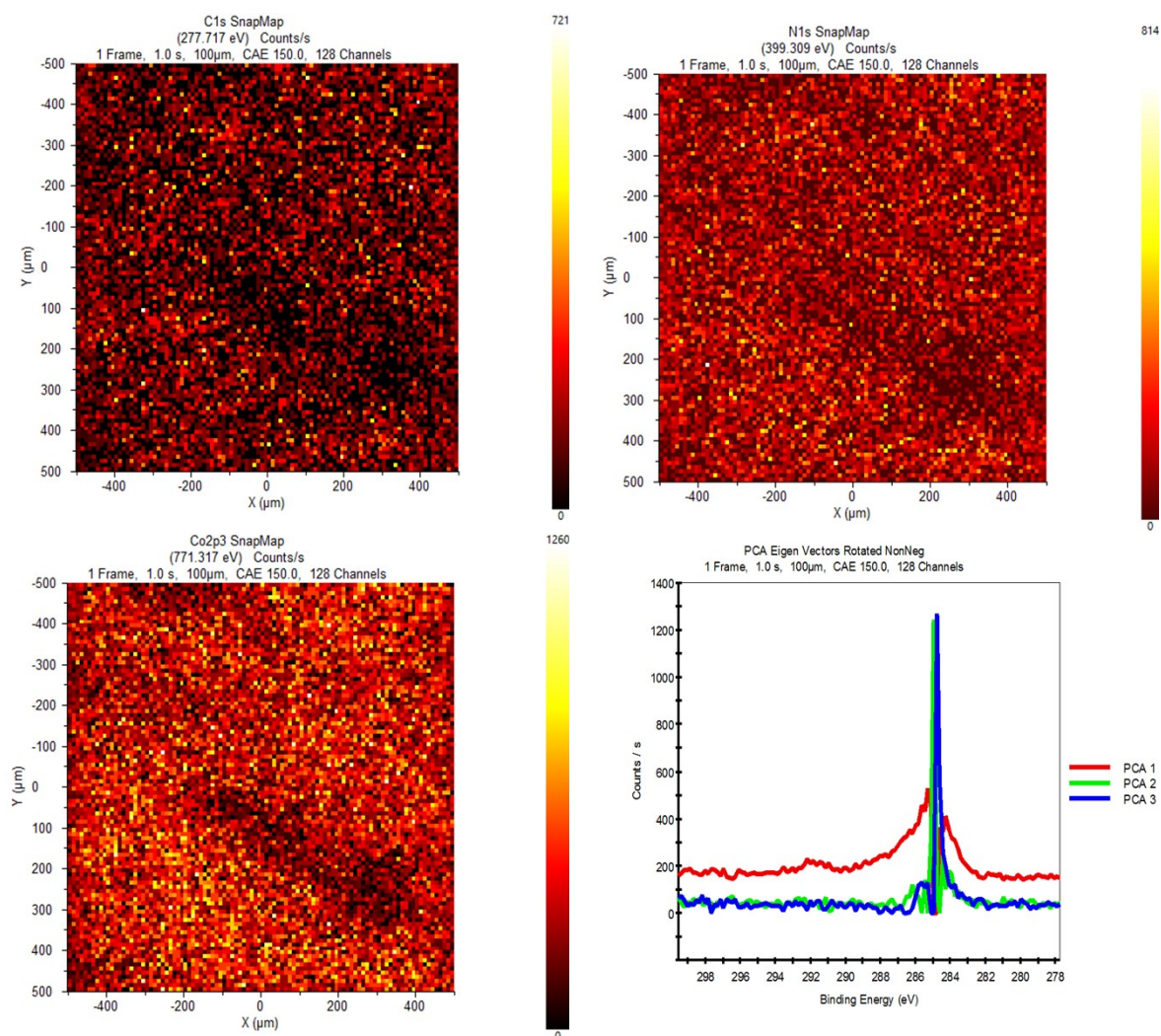
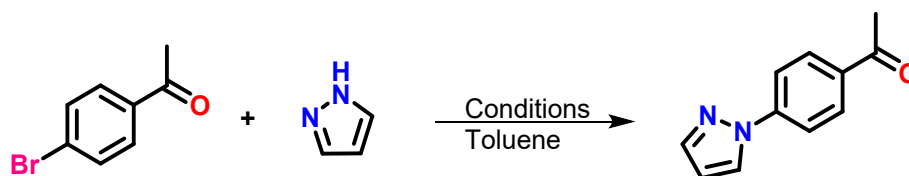


Figure S1. FE-SEM images of the Co@Apz@ASMNPs photocatalyst.



**Figure S2.** Principal Component Analysis (PCA) snapmap of Co@Apz@ASMNPs photocatalyst

**Table S1.** Optimization study to synthesize 1-(4-Acetylphenyl)-1*H*-pyrazole.



Entry	Catalyst (5 mol %)	Base (3 Equiv)	Additive (20 mol %)	T (°C)	Time (h)	Yield (%)
1.	-	K <sub>2</sub> CO <sub>3</sub>	-	120	19	23
2.	CuI	K <sub>2</sub> CO <sub>3</sub>	-	120	19	30
3.	CuI	K <sub>2</sub> CO <sub>3</sub>	1,2-Diaminocyclohexane	120	19	38
4.	CuI	K <sub>2</sub> CO <sub>3</sub>	Phenanthroline	120	19	45

5.	CuI	K <sub>3</sub> PO <sub>4</sub>	1,2-Diaminocyclohexane	120	19	65
6.	CuI	K <sub>3</sub> PO <sub>4</sub>	Phenanthroline	120	19	72

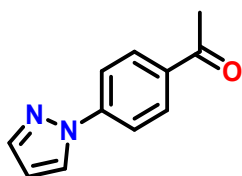
**Table S2.** C–H arylation of arenes utilizing various photoredox catalyst.



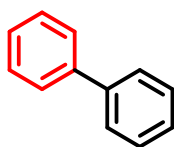
S.No	Catalyst	Conditions	Light source	Recyclability	Yield (%)	Ref.
1.	Fe(PLY-O,O) <sub>3</sub> (5 mol%)	K (20 mol%), DMSO, 36 h, RT		-	92	2
2.	Ferrocene (10 mol%)	Acetone, RT		-	81	3
3.	Ru(bpy) <sub>3</sub> (PF <sub>6</sub> ) <sub>2</sub> (0.5 mol%)	MeCN, RT, Ar		-	80	4
4.		Trifluoroacetic acid, Benzene, 120 h, rt	Blue led	-	72	5
5.	CpMn(CO) <sub>3</sub> (10 mol%)	DMSO, RT, 60 min	Blue led	-	68	6
6.	Cercosporin	Dimethyl sulfoxide; 16 h, rt	Sunlight	-	57	7
7.	Xanthone	Acetonitrile	UV light	-	87	8
8.	Xanthone	Acetonitrile; 20 °C	310 nm UV region	-	-	9
9.	Gallic acid	Acetone, Water; rt; 12 h, rt		-	50	10
10.	Immobilized Bodipy	Dimethyl sulfoxide; 12 h, 30 °C	Green LEDs	4	46	11
11.	1,1,2,2-Ethenetetramine, N1,N1,N1',N1', N2,N2,N2',N2'-octamethyl-, Oxonium, ethyl(9-methoxy-1H-phenalen-1-ylidene)-, tetrafluoroborate (1-) (1:1)	Dimethyl sulfoxide ; 12 h, RT		-	81	12

12.	Co@Apz@ASM NPs (35 mg)	DMSO, 12 h, N <sub>2</sub> , RT	White LEDs	4	75	<b>Th is wo rk</b>
-----	---------------------------	------------------------------------	---------------	---	----	--------------------------------

### <sup>1</sup>H and <sup>13</sup>C NMR data of the corresponding products

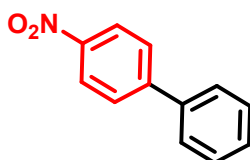


**1-(4-Acetylphenyl)-1H-pyrazole.**<sup>13</sup> <sup>1</sup>H NMR (400 MHz, CDCl<sub>3</sub>) δ 8.08 (d, *J* = 8.8 Hz, 2H), 8.04 (d, *J* = 2.5 Hz, 1H), 7.83 (d, *J* = 8.8 Hz, 2H), 7.79 (d, *J* = 1.3 Hz, 1H), 6.54 (t, *J* = 2.0 Hz, 1H), 2.65 (s, 3H); <sup>13</sup>C NMR (100 MHz, CDCl<sub>3</sub>) δ 197.0, 143.4, 142.1, 134.9, 130.1, 127.0, 118.5, 108.7, 26.7.



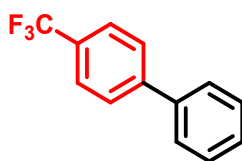
(3a)

**1,1'-biphenyl (3a).**<sup>14</sup> <sup>1</sup>H NMR (400 MHz, CDCl<sub>3</sub>) δ 7.67 (d, *J* = 8.0 Hz, 4H), 7.51 (t, *J* = 7.6 Hz, 4H), 7.42 (t, *J* = 7.3 Hz, 2H); <sup>13</sup>C NMR (100 MHz, CDCl<sub>3</sub>) δ 141.3, 128.8, 127.3, 127.2.



(3b)

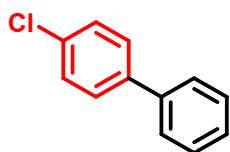
**4-nitro-1,1'-biphenyl (3b).**<sup>15</sup> <sup>1</sup>H NMR (400 MHz, CDCl<sub>3</sub>) δ 8.25 (d, *J* = 8.9 Hz, 2H), 7.70 (d, *J* = 8.9 Hz, 2H), 7.61 (d, *J* = 9.1 Hz, 2H), 7.51-7.42 (m, 3H); <sup>13</sup>C NMR (100 MHz, CDCl<sub>3</sub>) δ 147.6, 147.1, 138.9, 129.3, 129.1, 127.8, 127.5, 124.2.



(3c)

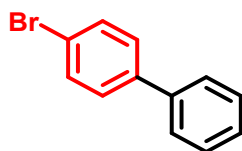
**4-(trifluoromethyl)-1,1'-biphenyl (3c).**<sup>16, 17</sup> <sup>1</sup>H NMR (400 MHz, CDCl<sub>3</sub>) δ 7.72 (d, *J* = 8.1 Hz, 4H), 7.65-7.63 (m, 2H), 7.54-7.44 (m, 3H); <sup>13</sup>C NMR (100 MHz, CDCl<sub>3</sub>) δ 144.9, 139.9,

129.3, 129.2, 129.0, 128.4, 127.6, 127.4, 125.9 (d,  $J = 3.8$  Hz), 123.2;  $^{19}\text{F}$  NMR (376 MHz,  $\text{CDCl}_3$ )  $\delta$  -62.154.



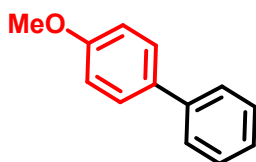
(3d)

**4-chloro-1,1'-biphenyl (3d).** $^{18}$   $^1\text{H}$  NMR (400 MHz,  $\text{CDCl}_3$ )  $\delta$  7.57 (dd,  $J = 14.1, 8.1$  Hz, 4H), 7.38-7.51 (m, 5H);  $^{13}\text{C}$  NMR (100 MHz,  $\text{CDCl}_3$ )  $\delta$  140.0, 139.7, 133.4, 128.9, 128.9, 128.4, 127.6, 127.0.



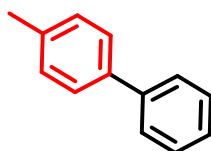
(3e)

**4-bromo-1,1'-biphenyl (3e).** $^{18}$   $^1\text{H}$  NMR (400 MHz,  $\text{CDCl}_3$ )  $\delta$  7.71-7.63 (m, 4H), 7.55-7.44 (m, 5H);  $^{13}\text{C}$  NMR (100 MHz,  $\text{CDCl}_3$ )  $\delta$  140.2, 140.0, 132.0, 129.0, 128.8, 127.8, 127.0, 121.6.



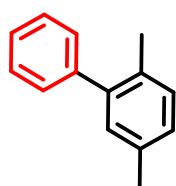
(3f)

**4-methoxy-1,1'-biphenyl (3f).** $^{14}$   $^1\text{H}$  NMR (400 MHz,  $\text{CDCl}_3$ )  $\delta$  7.60-7.55 (m, 4H), 7.45 (t,  $J = 7.6$  Hz, 2H), 7.34 (t,  $J = 7.4$  Hz, 1H), 7.01 (d,  $J = 8.8$  Hz, 2H), 3.89 (s, 3H);  $^{13}\text{C}$  NMR (100 MHz,  $\text{CDCl}_3$ )  $\delta$  159.1, 140.9, 133.8, 128.7, 128.2, 126.7, 126.6, 114.2, 55.36.



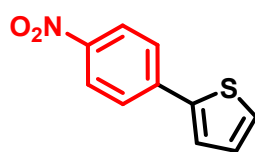
(3g)

**4-methyl-1,1'-biphenyl (3g).** $^{14}$   $^1\text{H}$  NMR (400 MHz,  $\text{CDCl}_3$ )  $\delta$  7.64 (d,  $J = 7.5$  Hz, 2H), 7.56 (d,  $J = 8.3$  Hz, 2H), 7.49 (t,  $J = 7.6$  Hz, 2H), 7.38 (t,  $J = 7.3$  Hz, 1H), 7.31 (d,  $J = 8.0$  Hz, 2H), 2.46 (s, 3H);  $^{13}\text{C}$  NMR (100 MHz,  $\text{CDCl}_3$ )  $\delta$  141.2, 138.4, 137.0, 129.5, 128.7, 127.0, 127.0, 21.14.



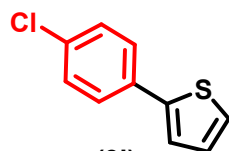
(3h)

**2,5-dimethyl-1,1'-biphenyl (3h).**<sup>19</sup> <sup>1</sup>H NMR (400 MHz, CDCl<sub>3</sub>)  $\delta$  7.42-7.38 (m, 2H), 7.34-7.30 (m, 3H), 7.16 (d,  $J$  = 7.4 Hz, 1H), 7.07 (d,  $J$  = 8.7 Hz, 2n), 2.34 (s, 3H), 2.23 (s, 3H); <sup>13</sup>C NMR (100 MHz, CDCl<sub>3</sub>)  $\delta$  142.2, 141.8, 135.2, 132.2, 130.6, 130.3, 129.2, 128.1, 128.0, 126.8, 21.0, 20.0.



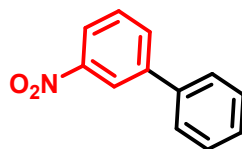
(3i)

**2-(4-nitrophenyl)thiophene (3i).**<sup>20, 21</sup> <sup>1</sup>H NMR (400 MHz, CDCl<sub>3</sub>)  $\delta$  8.25 (d,  $J$  = 8.8 Hz, 2H), 7.76 (d,  $J$  = 8.5 Hz, 2H), 7.46-7.50 (m, 2H), 7.17 (t,  $J$  = 4.4 Hz, 1H); <sup>13</sup>C NMR (100 MHz, CDCl<sub>3</sub>)  $\delta$  146.6, 141.6, 140.6, 128.7, 127.7, 126.0, 125.7, 124.4.



(3j)

**2-(4-chlorophenyl)thiophene (3j).**<sup>21, 22</sup> <sup>1</sup>H NMR (400 MHz, CDCl<sub>3</sub>)  $\delta$  7.57 (d,  $J$  = 8.5 Hz, 2H), 7.37 (d,  $J$  = 8.5 Hz, 2H), 7.33-7.31 (m, 2H), 7.11 (dd,  $J$  = 4.8, 3.9 Hz, 1H); <sup>13</sup>C NMR (100 MHz, CDCl<sub>3</sub>)  $\delta$  143.1, 133.2, 133.0, 129.0, 128.2, 127.1, 125.1, 123.5.



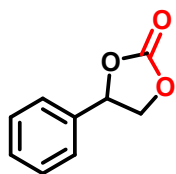
(3k)

**3-nitro-1,1'-biphenyl (3k).**<sup>18</sup> <sup>1</sup>H NMR (400 MHz, CDCl<sub>3</sub>)  $\delta$  8.46 (s, 1H), 8.21 (d,  $J$  = 8.3 Hz, 1H), 7.93 (d,  $J$  = 7.8 Hz, 1H), 7.64 (d,  $J$  = 7.3 Hz, 3H), 7.49 (dt,  $J$  = 24.7, 7.3 Hz, 3H); <sup>13</sup>C NMR (100 MHz, CDCl<sub>3</sub>)  $\delta$  148.7, 142.8, 138.6, 133.1, 129.8, 129.1, 128.6, 127.2, 122.0, 121.9.



(3)

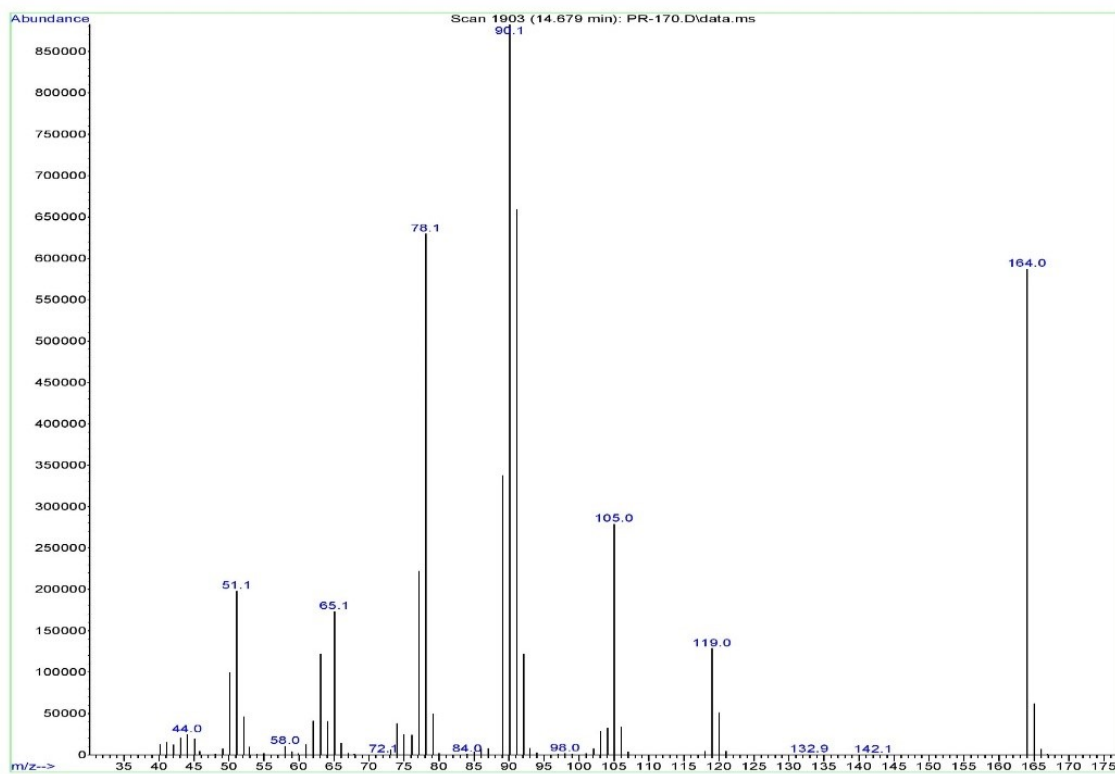
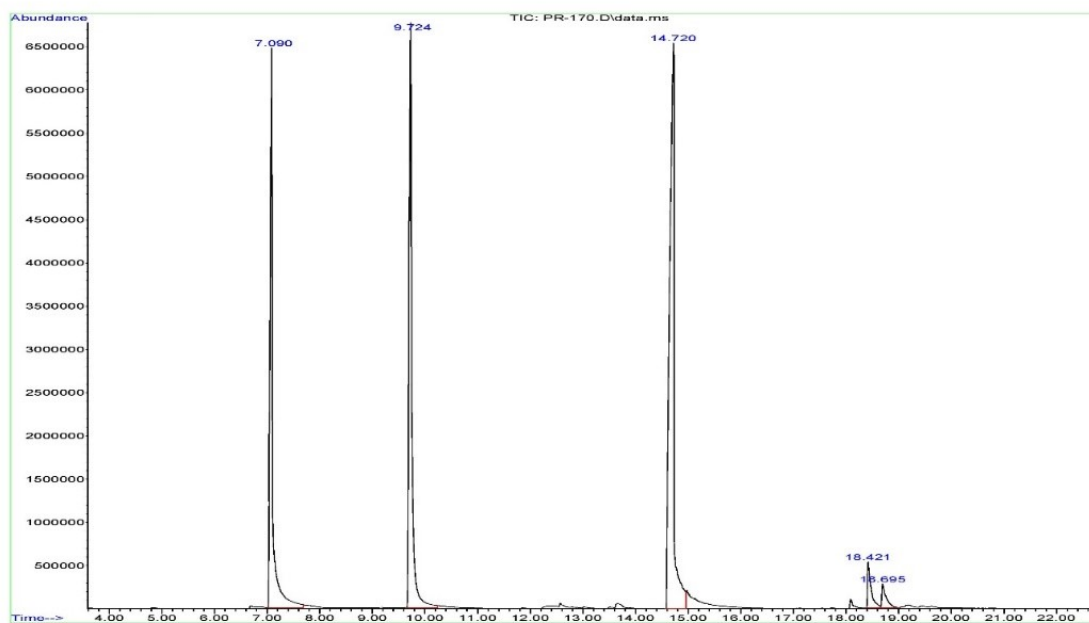
**2-nitro-1,1'-biphenyl (3).**<sup>14</sup> <sup>1</sup>H NMR (400 MHz, CDCl<sub>3</sub>)  $\delta$  7.88 (d,  $J$  = 8.0 Hz, 1H), 7.63-7.67 (m, 1H), 7.43-7.53 (m, 5H), 7.34-7.36 (m, 2H); <sup>13</sup>C NMR (100 MHz, CDCl<sub>3</sub>)  $\delta$  149.3, 137.4, 136.4, 132.3, 132.0, 128.7, 128.2, 128.2, 127.9, 124.1.



(5)

**4-phenyl-1,3-dioxolan-2-one (5).** Isolated Yield: 62%; <sup>1</sup>H NMR (400 MHz, CDCl<sub>3</sub>)  $\delta$  7.32-7.25 (m, 5H), 5.58 (t,  $J$  = 8.0 Hz, 1H), 4.68 (t,  $J$  = 8.5 Hz, 1H), 4.18 (dd,  $J$  = 8.6, 7.8 Hz, 1H); <sup>13</sup>C NMR (100 MHz, CDCl<sub>3</sub>)  $\delta$  155.2, 136.1, 129.7, 129.2, 126.2, 78.2, 71.3.

## GCMS Spectra



## References

1. G. Bartwal, M. Saroha and J. M. Khurana, *ChemistrySelect*, 2018, **3**, 12600-12602.
2. S. Chakraborty, J. Ahmed, B. K. Shaw, A. Jose and S. K. Mandal, *Chemistry—A European Journal*, 2018, **24**, 17651-17655.
3. S. Dixit, Q. T. Siddiqui, M. Muneer and N. Agarwal, *Tetrahedron Letters*, 2016, **57**, 4228-4231.

4. F. Gomes, V. Narbonne, F. Blanchard, G. Maestri and M. Malacria, *Organic Chemistry Frontiers*, 2015, **2**, 464-469.
5. M. C. Fürst, E. Gans, M. J. Böck and M. R. Heinrich, *Chemistry—A European Journal*, 2017, **23**, 15312-15315.
6. Y. F. Liang, R. Steinbock, L. Yang and L. Ackermann, *Angewandte Chemie*, 2018, **130**, 10785-10789.
7. S. Zhang, Z. Tang, W. Bao, J. Li, B. Guo, S. Huang, Y. Zhang and Y. Rao, *Organic & biomolecular chemistry*, 2019, **17**, 4364-4369.
8. S. Milanesi, M. Fagnoni and A. Albini, *Chemical communications*, 2003, 216-217.
9. S. Milanesi, M. Fagnoni and A. Albini, *The Journal of organic chemistry*, 2005, **70**, 603-610.
10. M. D. Perretti, D. M. Monzón, F. P. Crisóstomo, V. S. Martín and R. Carrillo, *Chemical communications*, 2016, **52**, 9036-9039.
11. R. Rajmohan, P. Nisha and P. Vairaprakash, *ACS omega*, 2019, **4**, 14458-14465.
12. J. Ahmed, S. Chakraborty, A. Jose and S. K. Mandal, *Journal of the American Chemical Society*, 2018, **140**, 8330-8339.
13. M. Taillefer, N. Xia and A. Ouali, *Angewandte Chemie International Edition*, 2007, **46**, 934-936.
14. M. J. Jin and D. H. Lee, *Angewandte Chemie International Edition*, 2010, **49**, 1119-1122.
15. G. Jonathan, *Chemical communications*, 2010, **46**, 2411-2413.
16. Y. Cheng, X. Gu and P. Li, *Organic letters*, 2013, **15**, 2664-2667.
17. Z. Xu, L. Gao, L. Wang, M. Gong, W. Wang and R. Yuan, *ACS Catalysis*, 2015, **5**, 45-50.
18. J. Wen, J. Zhang, S. Y. Chen, J. Li and X. Q. Yu, *Angewandte Chemie*, 2008, **120**, 9029-9032.
19. D. Liu, W. Gao, Q. Dai and X. Zhang, *Organic letters*, 2005, **7**, 4907-4910.
20. J.-H. Li, Y. Liang, D.-P. Wang, W.-J. Liu, Y.-X. Xie and D.-L. Yin, *The Journal of organic chemistry*, 2005, **70**, 2832-2834.
21. L. Zhi, H. Zhang, Z. Yang, W. Liu and B. Wang, *Chemical communications*, 2016, **52**, 6431-6434.
22. N. Kuhl, M. N. Hopkinson and F. Glorius, *Angewandte Chemie International Edition*, 2012, **51**, 8230-8234.